Available online at www.sciencedirect.com

ScienceDirect

journal homepage: www.elsevier.com/locate/he

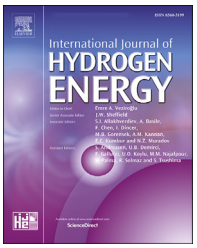

Comparison of well-to-wheels energy use and emissions of a hydrogen fuel cell electric vehicle relative to a conventional gasoline-powered internal combustion engine vehicle

Xinyu Liu [a,*], *Krishna Reddi* [a], *Amgad Elgowainy* [a], *Henning Lohse-Busch* [a], *Michael Wang* [a], *Neha Rustagi* [b]

[a] *Energy Systems Division, Argonne National Laboratory, 9700 S. Cass Avenue, Lemont, IL, 60439, USA*

[b] *Fuel Cell Technologies Office, U.S. Department of Energy, 1000 Independence Avenue SW, Washington, DC, 20585, USA*

HIGHLIGHTS

- Conducted well-to-wheels (WTW) analysis of H_2 fuel cell electric vehicle (HFCEV).
- Compared WTW result to that of gasoline internal combustion engine vehicle (ICEV).
- Incorporated both lab testing and window sticker fuel consumption data.
- HFCEV produces 15–45% less WTW greenhouse gas emissions compared to gasoline ICEV.
- WTW result is sensitive to electricity source for H_2 compression or liquefaction.

ARTICLE INFO

Article history:
Received 29 July 2019
Received in revised form
17 October 2019
Accepted 24 October 2019
Available online xxx

Keywords:
Hydrogen fuel cell electric vehicle
Well-to-Wheels
Life cycle analysis
Energy use
Emissions
Toyota Mirai

ABSTRACT

The operation of hydrogen fuel cell electric vehicles (HFCEVs) is more efficient than that of gasoline conventional internal combustion engine vehicles (ICEVs), and produces zero tailpipe pollutant emissions. However, the production, transportation, and refueling of hydrogen are more energy- and emissions-intensive compared to gasoline. A well-to-wheels (WTW) energy use and emissions analysis was conducted to compare a HFCEV (Toyota Mirai) with a gasoline conventional ICEV (Mazda 3). Two sets of specific fuel consumption data were used for each vehicle: (1) fuel consumption derived from the U.S. Environmental Protection Agency's (EPA's) window-sticker fuel economy figure, and (2) weight-averaged fuel consumption based on physical vehicle testing with a chassis dynamometer on EPA's five standard driving cycles. The WTW results show that a HFCEV, even fueled by hydrogen from a fossil-based production pathway (via steam methane reforming of natural gas), uses 5%–33% less WTW fossil energy and has 15%–45% lower WTW greenhouse gas emissions compared to a gasoline conventional ICEV. The WTW results are sensitive to the source of electricity used for hydrogen compression or liquefaction.

* *Corresponding author.*
E-mail address: xinyu.liu@anl.gov (X. Liu).

https://doi.org/10.1016/j.ijhydene.2019.10.192

Introduction

Hydrogen as a transportation fuel

Hydrogen (H_2) can be used to power automobiles with onboard H_2 fuel cells. H_2 fuel cell electric vehicles (HFCEVs) have a much higher energy conversion efficiency compared to gasoline conventional internal combustion engine vehicles (ICEVs), and produce zero tailpipe air pollutant emissions. On a well-to-wheels (WTW) basis, H_2 provides a clean alternative to gasoline and other petroleum derivatives [1]. Additionally, HFCEVs can be refueled within a few minutes and provide a customer refueling experience similar to that of conventional gasoline-powered vehicles. These characteristics position HFCEVs as prime candidates to address the growing demand for zero-emission vehicles, while also satisfying consumer expectations for short fueling time and a vehicle driving range similar to that experienced with conventional ICEVs powered by liquid hydrocarbon fuels.

A HFCEV consists of six major components: (1) H_2 storage tank, (2) air intake system, (3) fuel cell system, (4) power control unit, (5) battery, and (6) electric motor [1]. The chemical energy of H_2 is converted to electricity using the proton exchange membrane fuel cell technology. The H_2 from the onboard storage tank and oxygen from the air, supplied by the onboard air intake system, generate electricity via an electrochemical process as they pass through the fuel cell stack. The only byproduct of the process is water vapor, which is ejected from the fuel cell stack into the atmosphere. Therefore, during operation, a HFCEV does not have tailpipe emissions in the form of either greenhouse gas (GHG) or criteria air pollutants (CAPs). The electricity generated from the fuel cell is managed by the power control unit, which conditions and uses it as needed. The power control unit can either charge the battery, power the motor, or both, depending upon the operating condition or power demand of the HFCEV. Although the battery is not a major source of power for the HFCEV, it is used to store excess electricity, allow the fuel cell to operate near its peak efficiency, and support other functions of the vehicle. The electric motor converts the electric energy into mechanical energy, propelling the wheels.

In California, and other places like Japan and Europe, measures are already in place to support the adoption of HFCEVs; governments, in partnership with the private sector, have been funding the construction of H_2 refueling station networks for early adopters of HFCEVs. For example, the California Assembly Bill 8, "Alternative Fuel and Vehicle Technologies: Funding Programs," which was signed into law in September 2013, requires the California Energy Commission to provide $20 million per year for building an initial network of 100 H_2 refueling stations across the State of California [2], with a goal of 200 H_2 refueling stations by 2025 [3]. Japan has set a short-term target of deploying 40,000 HFCEVs on the road by early 2020, and ramping up to 200,000 HFCEVs by 2025. For the long term, Japan aims to enable 800,000 HFCEVs on the road by 2030. Japan also aims to expand the number of available H_2 fueling stations from 100 stations today to 160 by 2020, and 320 stations by 2025 [4,5]. The Japanese government has been promoting HFCEVs through regulatory reform, supporting technological developments and working with the private sector to develop H_2 stations [4]. Similar initiatives, such as H2USA in the United States [6], H_2 Mobility in Europe [7], and H_2 Alliance in China [8], have further demonstrated the interest in HFCEVs for transportation applications.

Although HFCEV operation has no associated tailpipe emissions, the H_2 stored onboard in the vehicle's tank may be associated with emissions in its production and delivery/refueling stages. Emissions are associated with the production of H_2 from various feedstocks, such as steam methane reforming (SMR) of natural gas, coal gasification, and electricity generation for water electrolysis [9]. The emissions associated with delivery/refueling occur at terminals and refueling stations. The GHG emissions associated with the H_2 production and delivery/refueling pathway can be estimated using a WTW analysis. The WTW analysis can be broken down into well-to-pump (WTP) and pump-to-wheels (PTW) stages, as shown in Fig. 1. The WTP stage includes fuel production from the primary source of energy (feedstock) through its delivery into the vehicle's energy storage system (fuel tank). The PTW stage includes fuel consumption during vehicle operation [10]. The results from WTP and PTW analyses are summed to give the WTW energy use and emissions on a fuel-cycle basis. Life cycle analysis (LCA) is a standardized tool for performing the WTW analysis and assessing the environmental impacts of a product "from cradle to grave," and it has already been applied to other types of transportation fuels [11].

H_2 production technologies

We evaluated two technology pathways for H_2 production, namely, SMR of natural gas and water electrolysis. In the SMR production pathway, methane from natural gas reacts with steam at high temperature (700–1000 °C) under a pressure of 3–25 bar in the presence of a catalyst to produce H_2, carbon monoxide, and a relatively small amount of carbon dioxide. This step is followed by the "water-gas shift reaction," where the carbon monoxide and steam react in the presence of a catalyst to produce carbon dioxide and additional H_2. In a third step, known as the "pressure-swing adsorption," carbon dioxide and other impurities are removed, leaving high-purity (>99.999%) H_2 for use in fuel cell applications [12].

SMR reaction:

$$CH_4 + H_2O + Heat \rightarrow CO + 3H_2$$

Water-gas shift reaction:

$$CO + H_2O \rightarrow CO_2 + H_2 + Heat$$

H_2 can also be produced via water electrolysis, which uses electricity to split water molecules into H_2 and oxygen. Electricity can be generated from different primary energy sources, e.g., coal, natural gas, nuclear, hydro, solar, and wind, by employing various power generation technologies. Currently, about 63% of the U.S. electric grid mix is generated from fossil sources [13], mostly coal and natural gas. Producing H_2 through electrolysis using the current grid mix of electricity may not reduce the WTW GHG emissions of

Please cite this article as: Liu X et al., Comparison of well-to-wheels energy use and emissions of a hydrogen fuel cell electric vehicle relative to a conventional gasoline-powered internal combustion engine vehicle, International Journal of Hydrogen Energy, https://doi.org/10.1016/j.ijhydene.2019.10.192

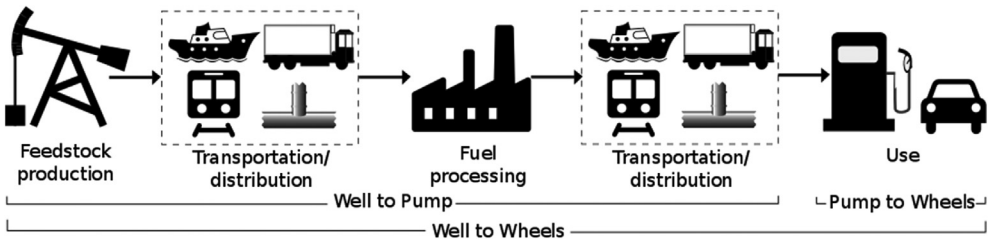

Fig. 1 – Well-to-wheels fuel cycle.

HFCEVs compared to baseline gasoline conventional ICEVs. However, electrolysis is a viable option for future production of H_2 when renewable sources dominate electricity generation, and where H_2 plays a major role in enabling higher penetration of renewables through its energy storage capacity. H_2 production at scale from non-fossil sources (e.g., wind, solar, hydro, and nuclear) can also enable cleaner use of energy in sectors other than transportation (e.g., power, industrial, and building).

H_2 delivery pathways

The H_2 delivery pathway starts at the production plant gate and ends at the HFCEV's onboard storage tank. The delivery pathway includes various processes, such as liquefaction or compression at a distribution terminal, transportation, and distribution, as well as compression, storage, precooling, and dispensing at a refueling station. H_2 is produced at a low pressure (~20 bar) from SMR and electrolysis processes, and may be compressed for transmission from the production plant to the distribution terminal via pipelines. However, in early HFCEV deployment markets, the demand for H_2 may not justify the commissioning of a dedicated H_2 pipeline network [14]. Therefore in the present study, we assumed that the central H_2 production plant is collocated with the distribution terminal. At the distribution terminal, the H_2 is either compressed or liquefied so that it can be loaded into compressed gaseous tube-trailers or cryogenic-liquid tankers for transportation to the refueling stations, as shown in Figs. 2 and 3, respectively [15].

Gaseous delivery pathway

For gaseous delivery of H_2 to refueling stations, H_2 may be compressed to a pressure between 200 and 500 bar and loaded onto gaseous tube-trailers for transportation and distribution (Fig. 2). The payload of the tube-trailer depends on the tube volume, number of tubes, and loading pressure, and is limited by the U.S. Department of Transportation's gross vehicle weight limit of 80,000 lb (36,287 kg). Currently, tube-trailers are configured to carry between 300 and 1100 kg of compressed gaseous hydrogen ($G.H_2$), which can be unloaded or swapped with an "empty" tube-trailer at the demand site. The tube-trailer at a refueling station supplies H_2 to a gaseous compressor, which compresses the H_2 to 1000 bar and stores it in a high-pressure buffer storage system for dispensing into vehicle tanks. The dispenser controls the flow from the high-pressure buffer storage into the vehicle tank using a refrigeration system that precools the H_2 to −40 °C to avoid overheating of the HFCEV tank.

Liquid delivery pathway

H_2 can be liquefied, typically using liquid nitrogen to precool the H_2 from ambient temperature to 80 K, followed by a series of compression and expansion processes to reach 20 K, the temperature necessary for H_2 liquefaction. The liquid hydrogen ($L.H_2$) is then loaded into large cryogenic storage

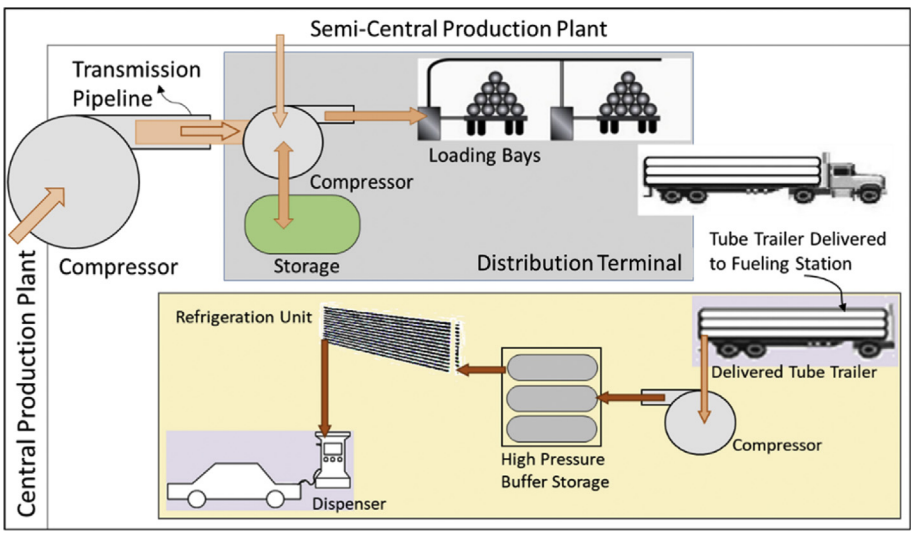

Fig. 2 – Schematic of the $G.H_2$ truck delivery pathway [15].

Please cite this article as: Liu X et al., Comparison of well-to-wheels energy use and emissions of a hydrogen fuel cell electric vehicle relative to a conventional gasoline-powered internal combustion engine vehicle, International Journal of Hydrogen Energy, https://doi.org/10.1016/j.ijhydene.2019.10.192

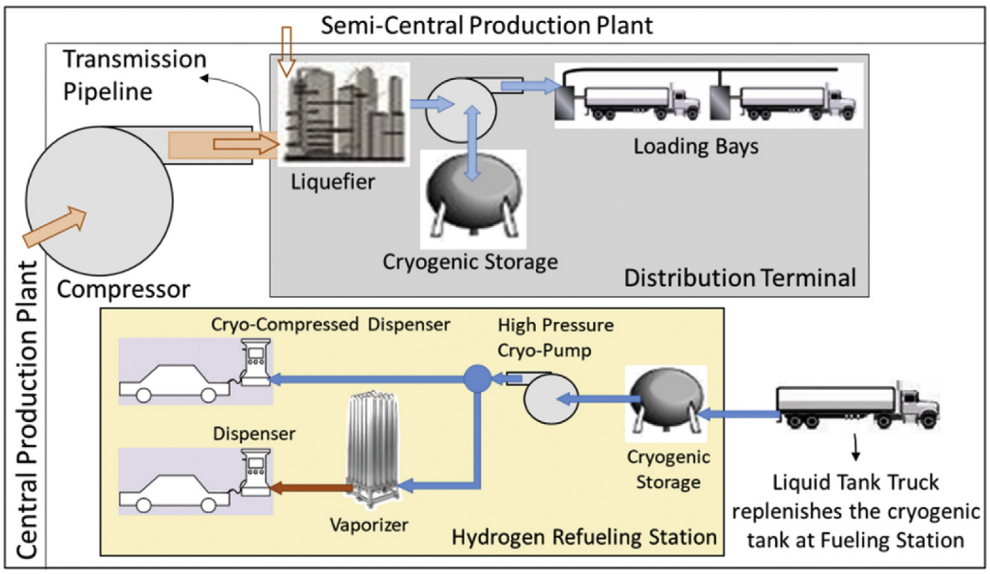

Fig. 3 – Schematic of the L.H_2 truck delivery pathway [15].

tanks at an adjacent distribution terminal, and subsequently dispensed into cryogenic-liquid tankers for delivery to refueling stations. A liquid tanker carries about 4 metric tons of L.H_2 payload near atmospheric temperature, for unloading into cryogenic tanks at one or more refueling stations. A refueling station's cryogenic tank stores H_2 at a pressure of 2–8 bar and supplies it to a high-pressure pump, which increases the pressure of H_2 to above 700 bar, heats the pressurized H_2 to −40 °C via a heat exchanger (known as a vaporizer), and dispenses it into the vehicle tank (Fig. 3). Alternatively, the cryo-pump may be used to directly pump the cryogenic H_2 into a cryo-compressed vehicle tank at 350 bar and −230 °C (Fig. 3). Cryo-compressed dispensing is currently in the demonstration phase. It promises to increase the HFCEV's onboard storage energy density, thus improving the driving range of HFCEVs [15].

L.H_2 delivery is, in general, more economical compared to compressed H_2 gas delivery in tube-trailers, especially for long transportation distances, owing to its higher payload (4 vs. 1 metric ton). However, the H_2 liquefaction process is energy-intensive, consuming between 11 and 15 kWh per kg of H_2, depending on H_2 supply pressure and the energy efficiency of the compression and expansion processes during liquefaction. Thus, it is important that the electricity used for liquefaction be of low cost and from low- or zero-carbon sources (e.g., nuclear or hydropower).

Vehicle testing on a chassis dynamometer

After it is dispensed into a HFCEV's onboard storage tank, H_2 is converted to electricity in the fuel cells to power the vehicle. In the present study, the fuel consumption data were based on the laboratory testing of standard certification drive cycles, as well as the data reported by www.fueleconomy.gov [16]. Argonne National Laboratory (Argonne) performed fuel economy (FE) testing of a 2016 Toyota Mirai HFCEV and a 2014 Mazda 3 i-ELOOP conventional ICEV on a chassis dynamometer [17]. Argonne's automotive test facility was built for powertrain research and technology assessment. The chassis dynamometer is housed in a thermal chamber, which allows testing under a range of real-world conditions. The test conditions are based on the U.S. Environmental Protection Agency (EPA) 5-cycle label FE procedures, which include ambient temperatures of −7 °C (20 °F), 25 °C (72 °F), and 35 °C (95 °F), with 850 W/m^2 of radiant solar emulation. The instrumentation on the vehicle was focused on measuring the power flows between the major powertrain components.

Testing was performed on a Toyota Mirai, which is a 114 kW fuel-cell-dominant hybrid electric vehicle. The measured peak efficiency is 66.0% and 63.7% for the stack and system, respectively. The Mazda 3 i-ELOOP is a conventional vehicle with a 2.5-L internal combustion engine and a 6-speed automatic transmission. The overall average powertrain efficiency on the U.S. city certification drive cycle (mild city driving) is 20.8% for the Mazda 3 conventional ICEV as compared to 64.7% for the Mirai fuel cell vehicle [17].

Prior LCA of HFCEV pathways

LCA of H_2 production and delivery pathways appears in the literature for a range of fuel cell vehicle classes, such as light-duty passenger vehicles [14,17–20], city buses [21–23], medium heavy-duty vehicles [24], and a fleet of various vehicle classes [25]. In these studies, the authors examined key factors impacting the life-cycle environmental performance of HFCEVs, such as the vehicle's FE, electricity generation mix, and H_2 delivery method. A wide range of studies examined the impact of FE of HFCEVs using reported literature values [18,26], dynamic vehicle simulation [21,24,27], and real-world operation data [23]. However, as pointed out by Ahmadi et al., driving patterns can have high impacts on HFCEVs' FE [19]. Therefore, the current study evaluated FE based on the weighting of different drive cycles (i.e., driving behaviors) to provide a better estimate of the fuel consumption customers can expect in the real-world driving of HFCEVs (Section Vehicle testing on a chassis dynamometer).

Please cite this article as: Liu X et al., Comparison of well-to-wheels energy use and emissions of a hydrogen fuel cell electric vehicle relative to a conventional gasoline-powered internal combustion engine vehicle, International Journal of Hydrogen Energy, https://doi.org/10.1016/j.ijhydene.2019.10.192

Lee et al. pointed out the importance of the electricity mix used for H_2 compression and/or liquefaction for LCA [24]. Lee et al.'s work suggested that under the average U.S. electricity generation mix, liquefaction and compression at refueling stations significantly increase WTW GHG emissions [24]. Similarly, Yoo et al. indicated that with the Korean grid mix, the water electrolysis pathway results in higher WTW GHG emissions compared to SMR, owing to the high CO_2 emission factor of the power generation mix [20]. The present study explores the impacts of various regional electricity generation mixes, and projected generation mix evolution, on the WTW GHG emissions of various H_2 production and delivery pathways.

Prior studies mostly applied literature values to capture the impacts of H_2 delivery, mostly in gaseous form. Few studies evaluated in detail the different H_2 delivery scenarios, which could considerably influence the WTW GHG emissions results for HFCEVs [24]. Moreover, as has been pointed out by Elgowainy et al., in the near term, H_2 will likely be transported via trucking, both in gaseous and liquid forms [14]. Therefore, this study provides a systematic comparison between these two delivery pathways (Section H_2 delivery pathways).

The present study compares WTW energy and emissions profiles for a light-duty conventional ICEV (Mazda 3) and a comparable HFCEV (Toyota Mirai) using two different methods for estimating FE, namely, the EPA-reported FE (at www.fueleconomy.gov) and the 5-cycle testing method. This study also evaluates the sensitivity of WTW energy use and emissions of HFCEVs to the source of electricity used for the H_2 compression or liquefaction. This study utilizes the Hydrogen Delivery Scenario Analysis Model (HDSAM) to capture the details of energy use in each step of H_2 delivery, and systematically compares the WTW emissions of gaseous and liquid deliveries.

Data and models

System boundary

In a complementary paper by Lohse-Busch et al. [17], vehicle operational (i.e., PTW) fuel consumption and emissions data were reported for a HFCEV (Toyota Mirai) and a comparable gasoline conventional ICEV (Mazda 3). In the present paper, we have expanded the system boundary to incorporate the effects of fuel production and delivery stages (i.e., WTP). We used Argonne's Greenhouse gas, Regulated Emissions, and Energy use in Transportation (GREET®) model to conduct the WTW analysis for various H_2 production and delivery pathways, and compared it to baseline gasoline conventional ICEVs [10]. We focused exclusively on the fuel cycle; i.e., the vehicle manufacturing cycle, including material extraction, vehicle component manufacturing, vehicle assembly, and vehicle recycling stages, is out of scope for this analysis. Estimates of vehicle manufacturing-cycle energy use and emissions can be found in other work [28].

We evaluated fuel production and delivery pathways for gasoline and H_2 to compare the WTW performance of the Toyota Mirai and Mazda 3. Gasoline is produced from crude-oil refining; thus, the energy consumption and emissions associated with its production are represented by the average of its processing units in U.S. refineries, and by the upstream crude recovery supplied to each refinery [29,30]. In this study, we assumed that E10 gasoline, which is a volumetric blend of 90% gasoline and 10% corn-ethanol, was combusted in the tests of the conventional ICEV.

In contrast, H_2 is mainly produced via SMR of natural gas. Currently, nearly half of the international H_2 demand is satisfied via this pathway [9]. However, as mentioned earlier, H_2 can also be produced via other production pathways, including water electrolysis. The environmental profile of the H_2 produced is significantly impacted by the energy source and conversion pathway. In this study, we focused on two pathways: (1) SMR of natural gas, because of its dominance in current H_2 production; and (2) water electrolysis via solar- or wind-based electricity, because of the growing interest in this pathway. In the SMR pathway, we assumed an energy conversion efficiency of 72% (lower heating value [LHV]-based), and accounted for the upstream processes of natural gas recovery, processing, and transmission/distribution to the H_2 production sites. For the water-electrolysis pathway, the H_2 production efficiency was assumed to be 66.8% [10], and we accounted for the upstream electricity generation pathways.

In this study, H_2 was assumed to be produced at the distribution terminal. It was also assumed to be delivered to refueling stations by either compressed gaseous tube-trailers or cryogenic-liquid tankers. We utilized the HDSAM to assess the energy use with various H_2 delivery scenarios [31].

For all H_2 delivery scenarios, the transportation distance between H_2 production site and refueling station was assumed to be 90 miles (60 miles for transmission from production gate to city gate, and 30 miles for distribution from city gate to refueling stations). Details of H_2 delivery assumptions and data used in this study are summarized in Table 1. Diesel fuel was used for transporting H_2 via trucks, and electricity was used for other processes, such as liquefaction, pumping, compression, and precooling. Table 1 suggests that compression is the biggest energy consumer in the G.H_2 delivery pathway, while liquefaction is the dominant energy consumer in the L.H_2 delivery pathway. Both processes consume electricity; therefore, the electricity source plays an important role in determining the environmental impacts of different H_2 delivery scenarios.

Window-sticker and 5-cycle test fuel consumption during vehicle operation

Vehicle fuel consumption (in Btu/mi) is defined by the fuel spent per unit distance traveled, and is calculated in this analysis by dividing the fuel's LHV (in Btu/gal for E10 gasoline, or Btu/kg for H_2) by vehicle FE (in mi/gal or mi/kg). Note that Btu is the British thermal unit, with 1 Btu = 1.055 kJ. The GREET default LHVs used in this analysis are 112,190 Btu/gal for E10 gasoline and 113,730 Btu/kg for H_2. One kilogram of H_2 contains approximately 1.4% more energy than a gallon of E10 gasoline.

EPA developed a 5-cycle label (i.e., window-sticker) FE to provide an estimate of the fuel consumption that customers could expect in the real-world driving of the cars they purchased. EPA developed the 5-cycle label FE equations on the

Please cite this article as: Liu X et al., Comparison of well-to-wheels energy use and emissions of a hydrogen fuel cell electric vehicle relative to a conventional gasoline-powered internal combustion engine vehicle, International Journal of Hydrogen Energy, https://doi.org/10.1016/j.ijhydene.2019.10.192

Table 1 – Energy use estimates for H_2 delivery pathways [31].

	$G.H_2$ via Tube-Trailer Truck		$L.H_2$ via Cryogenic Tanker Truck	
Characteristics	Payload (kg)	1000	Payload (kg)	4000
	Working Pressure (bar)	500	Working Pressure (bar)	
	Delivery Distance (mi)	90	Delivery Distance (mi)	90
At distribution terminal	Compression (kWh/kg H_2)	2.58	Liquefaction (kWh/kg H_2)	12
			Pumping (kWh/kg H_2)	0.08
During transportation	Fuel Use (MJ/kg H_2)	3.64	Fuel Use (MJ/kg H_2)	1.21
At refueling station	Compression (kWh/kg H_2)	1.21	Pumping (kWh/kg H_2)	0.55
	Pre-Cooling (kWh/kg H_2)	0.63		

basis of a comprehensive regression analysis, which fits phases of the existing certification drive cycles to match real-world FE [32]. However, it is worth mentioning that EPA has not applied the 5-cycle label FE equations to reported FE for the Toyota Mirai. This is because the Mirai is an alternative-fuel vehicle to which the alternative-fuel rule [33] is applicable. The official window-sticker FE information for both the Toyota Mirai HFCEV and the Mazda 3 conventional ICEV can be obtained from EPA's reporting in www.fueleconomy.gov [16].

Independently, Argonne conducted physical testing of both vehicles, based on EPA's 5-cycle label FE procedure, with a chassis dynamometer [17]. The 5-cycle label FE equations for city and highway FE were applied to both vehicles. The combined city/highway FE was obtained by applying EPA's rule of 55% city driving and 45% highway driving [32].

Table 2 summarizes the fuel consumption values for the Mazda 3 and Toyota Mirai as derived from EPA's window-sticker FE and 5-cycle test FE. The fuel consumption values based on the window-sticker FE are calculated using the official FE obtained from www.fueleconomy.gov [16]. and the GREET default LHVs for E10 gasoline and H_2; the 5-cycle test fuel consumption values are reported in Table A-2 of ref. [17].

WTW analysis using the GREET model

The GREET model utilizes the fuel consumption values shown in Table 2 to calculate the WTW results. The simulation year for upstream energy mixes for all fuel production pathways was specified to be 2018. The WTW environmental impacts of the Mazda 3 and Toyota Mirai were compared in terms of their fossil fuel consumption, GHG emissions, and CAP emissions. We considered CO and NO_x emissions as examples of CAP emissions, since both of them were measured during the tests conducted at Argonne [17].

EPA's assessment and categorization of tailpipe emissions are based on individual drive-cycle results, but for this study, the tailpipe emissions were intentionally processed through the 5-cycle label equations in order to maintain consistency with the FE calculation method.

Table 3 summarizes the emission results during the Mazda 3 vehicle operation test. The test GHG emission values were used to validate the ones provided by the GREET model. The test CAP emission values were adopted in this study, substituting for those provided by the GREET model. This is because the authors deemed the test results to be closer to reality in terms of CAP emissions. The operation of the Mirai (representative of HFCEVs) incurs zero tailpipe emissions.

As mentioned earlier, we considered two H_2 production pathways, namely, the SMR pathway and the water-electrolysis pathway using electricity from solar energy. We also examined two H_2 delivery pathways, namely, gas tube-trailer and cryogenic-liquid tanker deliveries. Thus, we analyzed a total of four technology pathways by combining the H_2 production and delivery pathways: SMR-based H_2 delivered via compressed gas tube-trailers (SMR $G.H_2$), SMR-based $L.H_2$ delivered via cryogenic-liquid tankers (SMR $L.H_2$), solar electrolysis-based H_2 delivered via compressed gas tube-trailers (Solar $G.H_2$), and solar electrolysis-based $L.H_2$ delivered via cryogenic-liquid tankers (Solar $L.H_2$). The delivered H_2 is supplied to a HFCEV (i.e., Toyota Mirai). The supplying of E10 gasoline to the conventional ICEV (i.e., the Mazda 3) is referred to as the gasoline pathway in the following discussion.

In addition, we assumed that the electricity used is sourced from the current average U.S. grid generation mix. Since the electricity source plays a critical role in determining the environmental profile of HFCEVs, various alternative sources have been assessed in this paper. Table 4 provides information on the fuel shares for the current and future U.S. and California (CA) average grid generation mixes. The fossil-fuel consumption and the GHG and CAP emission intensities for each fuel type are also provided.

Results and discussions

WTW fossil energy use and GHG emission results

Fig. 4 shows the WTW fossil energy use for the Mazda 3 (gasoline bars) and Toyota Mirai, in units of Btu/mile driven. In all four H_2 production and delivery pathways considered, the

Table 2 – Fuel consumption in Btu/mi for Toyota Mirai (model year 2016) and Mazda 3 (model year 2014).

Source	Toyota Mirai	Mazda 3
Window-sticker	1723	3568
5-cycle test	1937	3787

Table 3 – Test results for GHGs and CAP emissions of the Mazda 3, weighted per the EPA 5-cycle label equations.

Emission	CO_2	CH_4	NO_x	CO mid
Value (g/mile)	285.6	2.2E-03	5.5E-03	3.7E-01

Please cite this article as: Liu X et al., Comparison of well-to-wheels energy use and emissions of a hydrogen fuel cell electric vehicle relative to a conventional gasoline-powered internal combustion engine vehicle, International Journal of Hydrogen Energy, https://doi.org/10.1016/j.ijhydene.2019.10.192

Table 4 – Electricity generation fuel shares and fossil-fuel consumption and emission intensities for current (Year: 2018) and future (Year: 2030) U.S. and California (CA) grids [10].

Electricity source	U.S. Electricity Mix Share		CA Electricity Mix Share		Energy and Emission Intensities per 1 kWh of Electricity at Wall Outlet (2018 U.S. generation mix)			
	2018	2030	2018	2030	Fossil-fuel consump-tion (Btu)	GHGs (g)	CO (g)	NO_x (g)
Residual Oil	0.5%	0.2%	0.0%	0.0%	1.19E+04	1.03E+03	2.55E-01	4.48E+00
Natural Gas	29.8%	33.0%	41.3%	27.4%	7.78E+03	5.07E+02	3.49E-01	4.31E-01
Coal	32.7%	28.2%	6.3%	0.0%	1.02E+04	1.06E+03	8.72E-02	5.14E-01
Nuclear	20.6%	16.6%	9.7%	0.0%	9.87E+01	8.32E+00	1.30E-02	1.76E-02
Biomass	0.1%	0.2%	0.5%	1.6%	4.09E+02	6.52E+01	4.99E+00	1.10E+00
Hydro	7.7%	7.1%	17.9%	17.6%	0.00E+00	0.00E+00	0.00E+00	0.00E+00
Geothermal	0.4%	1.0%	5.0%	14.0%	0.00E+00	9.57E+01	0.00E+00	0.00E+00
Wind	6.4%	9.7%	7.1%	15.3%	0.00E+00	0.00E+00	0.00E+00	0.00E+00
Solar	1.2%	3.4%	11.1%	22.8%	0.00E+00	0.00E+00	0.00E+00	0.00E+00
Others (e.g., pumped storage)	0.5%	0.6%	1.2%	1.4%	0.00E+00	2.61E+00	0.00E+00	0.00E+00

WTW fossil energy use calculated from the window-sticker FE-based fuel consumption value is approximately 11% less than that calculated using the 5-cycle test fuel consumption value. This difference is in line with that provided in Table 2, since the window-sticker fuel consumption is 11% less than the 5-cycle test result for the Toyota Mirai. This difference is due partly to the application of different methods (i.e., alternative-fuel rule and 5-cycle label FE equations) to calculate the fuel consumption of the Toyota Mirai, and partly due to acceptable test deviations. The rest of the discussion focuses on the 5-cycle test results. Under this scenario, the raw test results for both vehicles are processed through the 5-cycle label equations for consistent comparison of the Toyota Mirai and Mazda 3. The results based on the window-sticker fuel consumption are also provided to complete the analysis.

Fig. 4 also indicates that the Toyota Mirai powered by SMR-based H_2 requires only 55% of the fossil-energy consumed by the Mazda 3 during the vehicle operational stage. For conventional ICEVs, the vehicle operation (i.e., PTW) stage accounts for 78% of the WTW fossil-energy consumption. For the HFCEV operation stage, the SMR-based H_2 still counts towards fossil-energy consumption, since the origin of the consumed H_2 is natural gas, which is a fossil fuel. On the other hand, H_2 produced from the solar-based water-electrolysis pathway does not contribute to fossil-energy consumption during the vehicle operation stage, since solar energy is renewable (i.e., non-fossil).

Fig. 4 suggests that even for the solar-based H_2 pathways, there exists some fossil-fuel consumption during the WTP stage. This consumption is due to the use of fossil-based U.S. average electricity mix along the H_2 production and delivery pathways (e.g., for liquefaction, compression, and precooling). As shown in Table 1, to deliver 1 kg of H_2, the gaseous pathway requires 4.42 kWh of electricity for compression and precooling, while the liquid pathway requires 12.55 kWh of electricity for liquefaction and pumping. This electricity is assumed to be sourced from the 2018 U.S. average grid generation mix, with 30% of the electricity from natural gas and

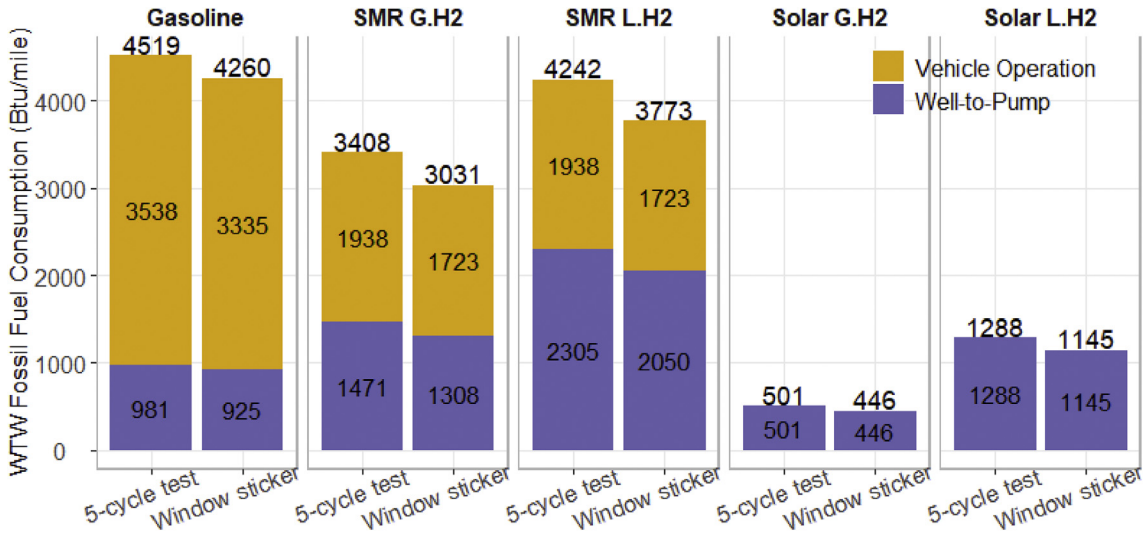

Fig. 4 – WTW fossil energy use for Mazda 3 (gasoline bars) and Toyota Mirai. (The WTW results are marked at the top of the bar; the WTP and vehicle operation results are marked in the middle of the corresponding stacked bars. The same applies to Figs. 5–7).

Please cite this article as: Liu X et al., Comparison of well-to-wheels energy use and emissions of a hydrogen fuel cell electric vehicle relative to a conventional gasoline-powered internal combustion engine vehicle, International Journal of Hydrogen Energy, https://doi.org/10.1016/j.ijhydene.2019.10.192

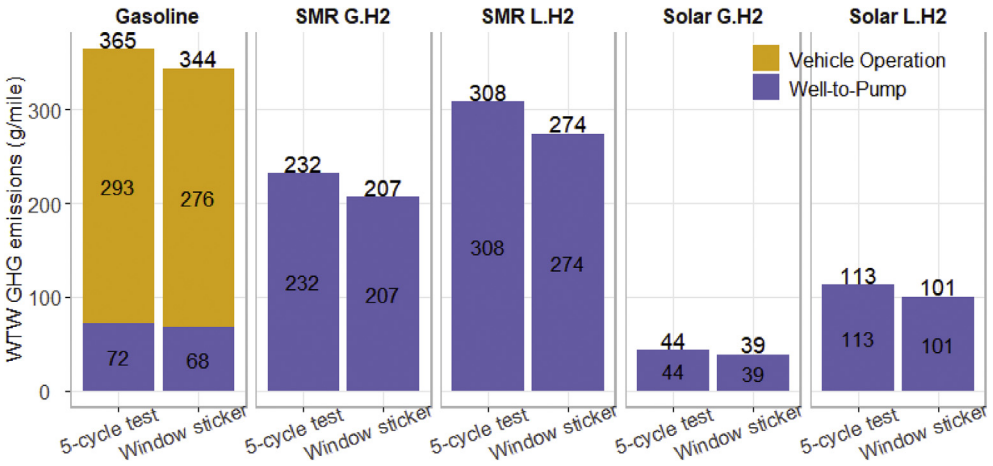

Fig. 5 – WTW GHG emissions for Mazda 3 (gasoline bars) and Toyota Mirai.

33% from coal. The liquid delivery pathway incurs more WTW fossil-energy use, since it consumes more electricity, over 60% of which is based on non-renewable resources.

Fig. 5 shows the WTW GHG emissions for the Mazda 3 (gasoline bars) and Toyota Mirai. The trends in WTW GHG emissions follow those of fossil-energy consumption in Fig. 4. The only difference is that the Mirai does not emit GHG during the operation stage. For HFCEVs, the only emission from the tailpipe is water vapor.

When the Toyota Mirai and Mazda 3 are compared in terms of their WTW GHG emissions under the 5-cycle test fuel consumption scenario, the Mazda 3 produces more emissions than the Toyota Mirai under all H_2 production and delivery scenarios. Even in the worst scenario (SMR L.H_2), the Toyota Mirai shows a 16% reduction in GHG emissions compared with the Mazda 3; in the best scenario (Solar G.H_2), this reduction is 88%.

Criteria air pollutant emissions results

Fig. 6 shows the WTW CO emissions for the Mazda 3 (gasoline bars) and Toyota Mirai. For gasoline conventional ICEVs, approximately 85% of the CO is emitted during the operational stage, owing to the incomplete combustion of gasoline in the engine. For HFCEVs, no CO is emitted during the operation stage, since H_2 is a zero-carbon fuel. In terms of the vehicles' WTW CO emissions under the 5-cycle test fuel consumption scenario, the Mazda 3 performs worse than the Toyota Mirai under all H_2 production and delivery scenarios. Under the best scenario (Solar G.H_2), the Mirai exhibits a 96% CO reduction; even under the worst scenario (SMR L.H_2), the Mirai still maintains an 80% CO reduction compared to the Mazda 3.

Fig. 7 shows the WTW NO_x emissions for the Mazda 3 (gasoline bars) and Toyota Mirai. Under the 5-cycle test fuel consumption scenario, the Mirai's consumption of H_2 from the SMR liquid pathway results in 7% more NO_x emissions than the Mazda 3, mainly because the U.S. electricity generation mix was assumed to be used for H_2 liquefaction: 33% of the 2018 U.S. grid generation was fueled by coal, with 0.5 g NO_x emitted for each kWh of coal-based electricity produced (Table 4). It is also worth mentioning that for HFCEVs, the vehicle operation stage does not result in NO_x emissions, whereas the upstream (i.e., electricity generation) emissions usually occur in non-urban settings, i.e., with lower impacts on population compared to vehicle tailpipe emissions.

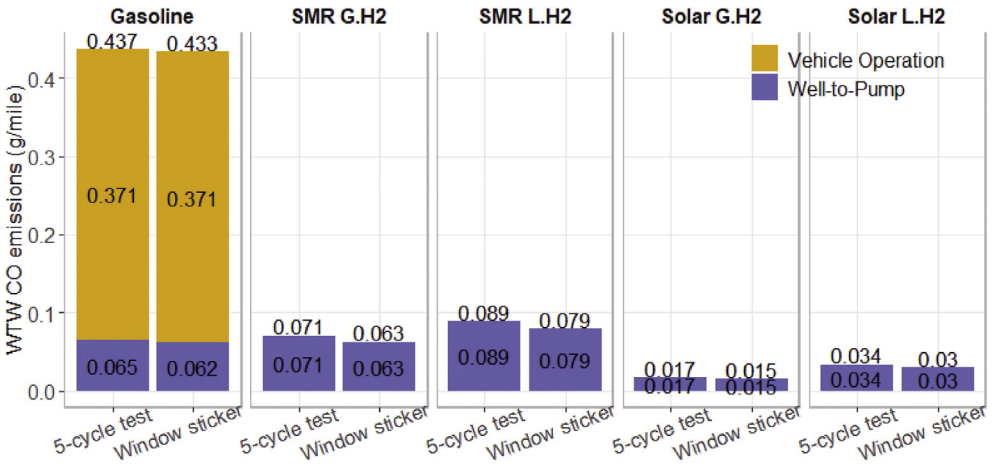

Fig. 6 – WTW CO emissions for Mazda 3 (gasoline bars) and Toyota Mirai.

Please cite this article as: Liu X et al., Comparison of well-to-wheels energy use and emissions of a hydrogen fuel cell electric vehicle relative to a conventional gasoline-powered internal combustion engine vehicle, International Journal of Hydrogen Energy, https://doi.org/10.1016/j.ijhydene.2019.10.192

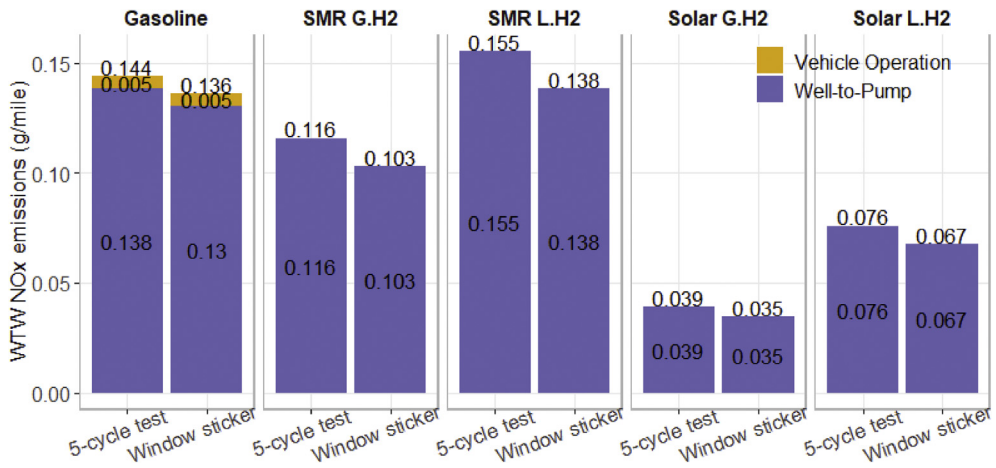

Fig. 7 – WTW NO_x emissions for Mazda 3 (gasoline bars) and Toyota Mirai.

Impact of electricity generation mix on WTW energy use and emissions

As presented in Table 1, to deliver 1 kg of L.H_2, 12 kWh of electricity is needed for the liquefaction process alone, which is almost three times as high as the total electricity requirement for gaseous delivery. Therefore, the environmental profile of the L.H_2 pathway is heavily dependent on the source of the electricity being consumed.

In this study, we assumed the H_2 liquefaction energy source to be the 2018 U.S. average electricity grid generation mix. We also considered two additional electricity

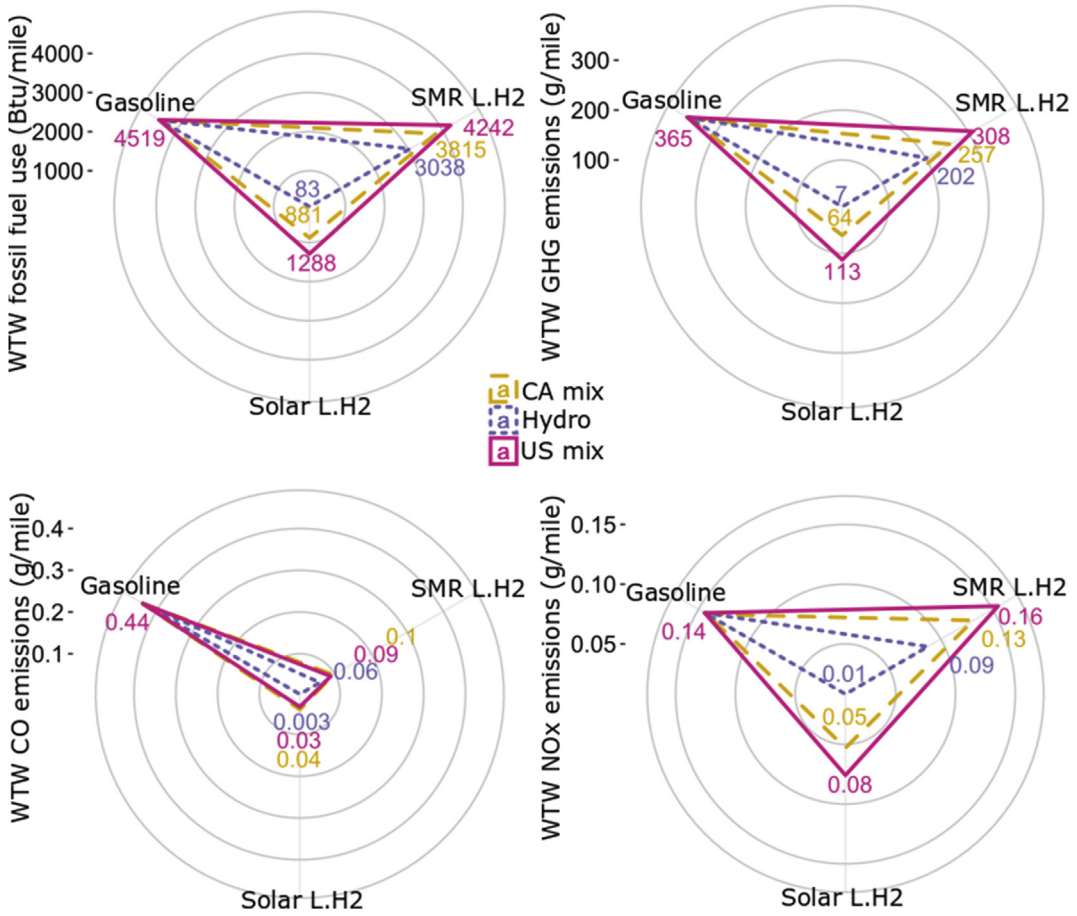

Fig. 8 – WTW fossil-energy use and emissions for modeling H_2 liquefaction energy with various electricity alternatives under the 5-cycle test fuel consumption scenario.

Please cite this article as: Liu X et al., Comparison of well-to-wheels energy use and emissions of a hydrogen fuel cell electric vehicle relative to a conventional gasoline-powered internal combustion engine vehicle, International Journal of Hydrogen Energy, https://doi.org/10.1016/j.ijhydene.2019.10.192

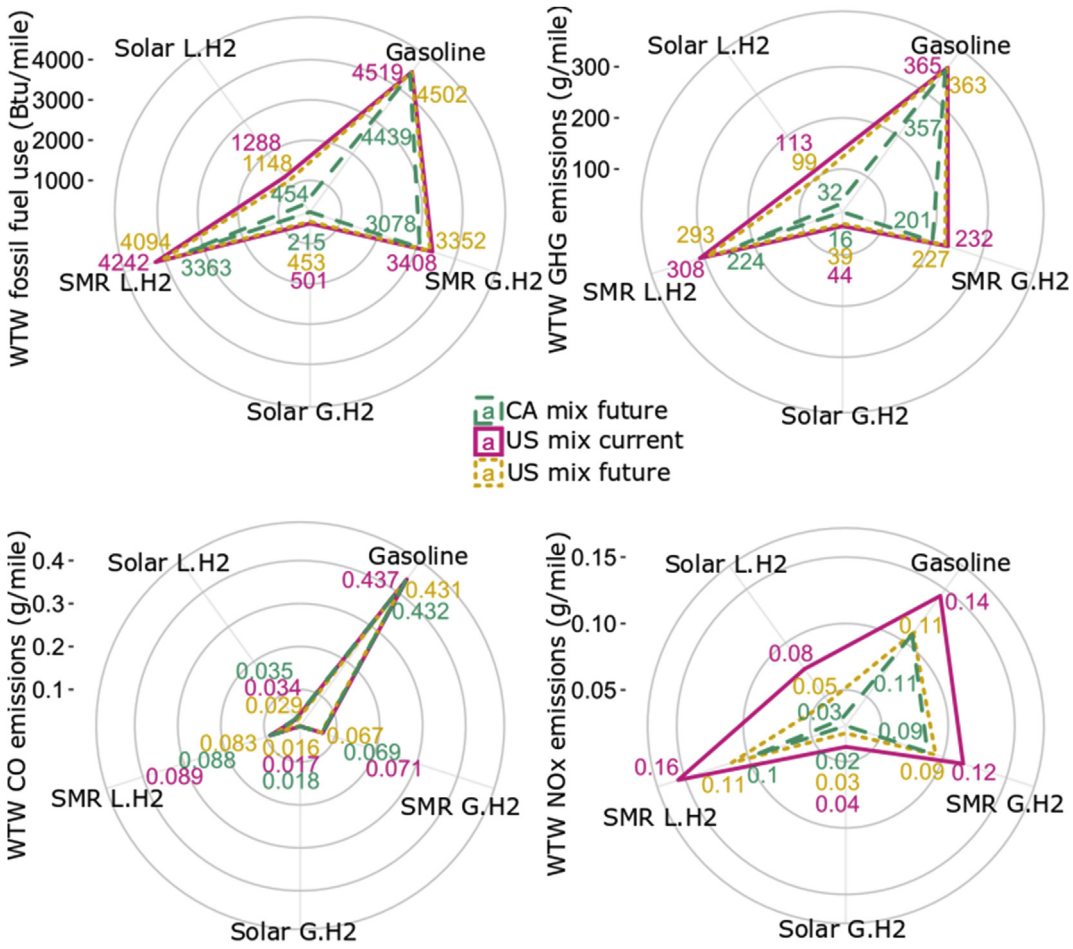

Fig. 9 – Potential effects of electricity-mix evolution on WTW results under the 5-cycle test fuel consumption scenario.

generation alternatives: 1) The CA grid generation mix for H_2 liquefaction; under this scenario, we assumed that the rest of the electricity consumed in the WTW life cycle was also sourced from the CA grid. In the 2018 grid, 48% of electricity generation in CA originated from fossil sources, while the U.S. grid mix was 63% fossil-based. 2) Hydro-based electricity for H_2 liquefaction; under this scenario, we assumed that the rest of the electricity was sourced from the 2018 U.S. grid mix.

Fig. 8 shows the environmental footprints of the Toyota Mirai (SMR, solar) and Mazda 3 (gasoline) under the above electricity generation scenarios. The H_2 pathways based on gaseous delivery are excluded from the figure, since we have only varied the liquefaction energy source. The WTW results as a whole are plotted, instead of breaking them down into WTP and vehicle operation stages. This approach was taken because the change in electricity source would only affect the energy consumption and emissions during the WTP stage, since the vehicle operation stage does not consume external electricity. Electricity alternatives have minor impact on conventional ICEVs' environmental performance, since most of the fossil-energy consumption and GHG and CAP emissions occur during the vehicle operation stage.

Shifting the energy for H_2 liquefaction from the U.S. to the CA grid mix reduces the fossil-energy use for the SMR L.H_2 pathway by 427 Btu/mile. For the Solar L.H_2 pathway, switching the energy for H_2 liquefaction from the U.S. grid mix to hydro-based electricity and the CA grid mix reduces the WTW fossil-energy consumption by 94% and 32%, respectively.

Similarly, for the Solar L.H_2 pathway, shifting from the U.S. mix to hydro-based electricity for H_2 liquefaction reduces the GHG emissions by 106 g/mile. Therefore, if the Toyota Mirai utilizes H_2 from this pathway, the GHG reduction can be as high as 358 g per mile compared to the Mazda 3.

With respect to CAPs, the SMR L.H_2 pathway shows slightly more NO_x emissions (0.16 g/mile) than the gasoline pathway (0.14 g/mile), if the electricity for H_2 liquefaction is sourced from the average U.S. grid mix. However, if hydro-based electricity is used for H_2 liquefaction, the WTW NO_x emission of the SMR L.H_2 pathway is reduced from 0.16 to 0.09 g/mile. Thus, the electricity source can affect the environmental footprint of HFCEVs, especially for the L.H_2 pathways.

Sourcing electricity from the CA grid instead of the U.S. grid slightly increases CO emissions for L.H_2 pathways. This is because the CA mix has more electricity from natural gas (41.3%) compared to the U.S. mix (29.8%). However, the WTW

Please cite this article as: Liu X et al., Comparison of well-to-wheels energy use and emissions of a hydrogen fuel cell electric vehicle relative to a conventional gasoline-powered internal combustion engine vehicle, International Journal of Hydrogen Energy, https://doi.org/10.1016/j.ijhydene.2019.10.192

CO emissions for the Solar L.H_2 pathway can be as low as 0.003 g/mile if hydro-based electricity is used for liquefaction, resulting in a 99% CO reduction for the Toyota Mirai compared to the Mazda 3.

Impact of evolving electricity grid mix on WTW energy use and emissions

The GREET model provides electricity mix predictions for the U.S. and CA grids up to year 2050, based on the Energy Information Administration's Annual Energy Outlook [13]. In this study, we compared the WTW results using the current (2018) and future (2030) electricity grid generation mixes, which are reported in Table 4. In year 2030, coal-based electricity is eliminated from the CA grid, and the share of natural gas-based electricity is reduced to 27.4%. The rest of the electricity in the future CA grid is based on renewable resources, such as biomass, hydro, solar, and wind. Therefore, it should be expected that the WTW fossil-energy use would decrease over time as the electricity source shifts from the current U.S. grid mix to the future CA grid mix (Fig. 9). However, there is only a slight reduction in fossil-energy consumption when shifting from the current to the future U.S. grid mix, as the 2030 U.S. grid sources less electricity from coal but relies more on natural gas.

The trends in GHG emissions track well with those of fossil-energy consumption. For example, after a shift from the current U.S. mix to the future CA mix, the Solar L.H_2 pathway consumes 65% less fossil-energy and emits 72% less GHGs. Within the context of the future CA grid mix, there would be an approximately 90% reduction in both WTW fossil-energy use and GHG emissions for the Toyota Mirai using L.H_2 from the solar pathway compared to the Mazda 3. In terms of NO_x emissions, the future CA grid mix reduces NO_x emissions because of the elimination of coal-based electricity. Thus, within the context of the future CA grid mix, the Toyota Mirai outperforms the Mazda 3 in all criteria considered in this analysis, even if it is fueled by H_2 from the SMR liquid pathway, which has the highest environmental impacts.

Conclusions

This paper compared the WTW energy use and emissions of the Toyota Mirai HFCEV with those of the Mazda 3 conventional ICEV, with two sets of data on specific fuel consumption: (1) fuel consumption based on EPA's window-sticker FE reported in www.fueleconomy.go, and (2) fuel consumption data measured at Argonne and reported by Lohse-Busch et al. [17]. The WTW results show that a HFCEV, even fueled by H_2 from a fossil-based production pathway (via SMR of natural gas), exhibits 5%–33% lower WTW fossil-energy use and 15–45% lower WTW GHG emissions than a gasoline conventional ICEV. The WTW results are sensitive to the source of electricity used for compression or liquefaction of H_2. The worst-case scenario for a HFCEV is the SMR L.H_2 pathway, assuming a U.S. average electricity grid generation mix for H_2 liquefaction. Yet this pathway provides a 15% reduction in GHG emissions compared to the gasoline conventional ICEV. WTW CAP emissions for HFCEVs also depend strongly on the electricity used for compression or liquefaction. Within the context of the future CA or U.S. average electricity grid generation mix, a HFCEV produces less CO and NO_x emissions than a gasoline conventional ICEV.

Acknowledgments

This research was supported by the Fuel Cell Technologies Office of the U.S. Department of Energy's Office of Energy Efficiency and Renewable Energy under Contract No. DE-AC02-06CH11357. The authors thank Fred Joseck from DOE's Fuel Cell Technologies Office for his guidance and support. The views and opinions of the authors expressed herein do not necessarily state or reflect those of the United States Government or any agency thereof. Neither the United States Government nor any agency thereof, nor any of their employees, makes any warranty, expressed or implied, or assumes any legal liability or responsibility for the accuracy, completeness, or usefulness of any information, apparatus, product, or process disclosed, or represents that its use would not infringe privately owned rights.

REFERENCES

[1] Reddi K, Elgowainy A, Wang M. Special section: energy - fuel cells for mobile applications. Chem Eng Prog 2016, July:50–4.
[2] Berner J, Martinez A. Joint agency staff report on assembly Bill 8. https://cafcp.org/sites/default/files/2018-AB-8-Joint-Report-Presentation-CaFCP-2019-02-14.pdf. [Accessed 10 June 2019].
[3] California Fuel Cell Partnership. The California fuel cell revolution: a vision for advancing economic, social and environmental priorities. https://cafcp.org/sites/default/files/CAFCR.pdf. [Accessed 10 June 2019].
[4] Ministerial Council on Renewable Energy Hydrogen and Related Issues. Basic hydrogen strategy. https://www.meti.go.jp/english/press/2017/pdf/1226_003b.pdf. [Accessed 10 June 2019].
[5] Ministry of Economy, Trade, and Industry, Japan. The strategy road map for hydrogen and fuel cells: industry-academia-government action plan to realize "hydrogen society. https://www.meti.go.jp/press/2018/03/20190312001/20190312001-3.pdf. [Accessed 10 June 2019].
[6] H2USA. https://www.h2usa.org. [Accessed 30 September 2019].
[7] Hydrogen mobility Europe. https://h2me.eu. [Accessed 4 September 2019].
[8] China Hydrogen Alliance. http://www.h2cn.org/en/dynamics.html. [Accessed 4 September 2019].
[9] Kalamaras CM, Efstathiou AM. Hydrogen production technologies: current state and future developments. Conf Pap Energy 2013:690627. https://doi.org/10.1155/2013/690627.
[10] Energy Systems. Argonne national laboratory. The greenhouse gases, regulated emissions, and energy use in transportation (GREET) model. https://greet.es.anl.gov. [Accessed 16 April 2019].
[11] Liu X, Singh S, Gibbemeyer EL, Tam BE, Urban RA, Bakshi BR. The carbon-nitrogen nexus of transportation fuels. J Clean Prod 2018;180:790–803. https://doi.org/10.1016/J.JCLEPRO.2018.01.090.

Please cite this article as: Liu X et al., Comparison of well-to-wheels energy use and emissions of a hydrogen fuel cell electric vehicle relative to a conventional gasoline-powered internal combustion engine vehicle, International Journal of Hydrogen Energy, https://doi.org/10.1016/j.ijhydene.2019.10.192

[12] Sun P, Young B, Elgowainy A, Lu Z, Wang M, Morelli B, et al. Criteria air pollutants and greenhouse gas emissions from hydrogen production in U.S. Steam methane reforming facilities. Environ Sci Technol 2019;53(12):7103–13. https://doi.org/10.1021/acs.est.8b06197.

[13] U.S. Energy Information Administration (EIA). Annual energy Outlook. https://www.eia.gov/outlooks/aeo. [Accessed 10 June 2019].

[14] Elgowainy A, Han J, Ward J, Joseck F, Gohlke D, Lindauer A, et al. Cradle-to-Grave lifecycle analysis of U.S. Light duty vehicle-fuel pathways: a greenhouse gas emissions and economic assessment of current (2015) and future (2025-2030) technologies. IL (United States): Argonne; 2016. https://doi.org/10.2172/1254857.

[15] Reddi K, Mintz M, Elgowainy A, Sutherland E. Challenges and opportunities of hydrogen delivery via pipeline, tube-trailer, LIQUID tanker and methanation-natural gas grid. Chap. 35. In: Stolten D, Emonts B, editors. Hydrogen science and engineering: materials, processes, systems and technologies. Weinheim, Germany: Wiley-VCH Verlag GmbH & Co. KGaA; 2016. p. 849–74. https://doi.org/10.1002/9783527674268.ch35.

[16] U.S. Department of Energy. Office of energy efficiency & renewable energy. www.fueleconomy.gov. [Accessed 17 April 2019]. https://www.fueleconomy.gov.

[17] Lohse-Busch H, Stutenberg K, Duoba M, Liu X, Elgowainy A, Wang M, et al. Automotive fuel cell stack and system efficiency and fuel consumption based on vehicle testing on a chassis dynamometer at minus 18°C to positive 35°C temperatures. Int J Hydrog Energy 2019. https://doi.org/10.1016/j.ijhydene.2019.10.150.

[18] Ahmadi P, Kjeang E. Comparative life cycle assessment of hydrogen fuel cell passenger vehicles in different Canadian provinces. Int J Hydrogen Energy 2015;40:12905–17. https://doi.org/10.1016/J.IJHYDENE.2015.07.147.

[19] Ahmadi P, Torabi SH, Afsaneh H, Sadegheih Y, Ganjehsarabi H, Ashjaee M. The effects of driving patterns and PEM fuel cell degradation on the lifecycle assessment of hydrogen fuel cell vehicles. Int J Hydrogen Energy 2019. https://doi.org/10.1016/J.IJHYDENE.2019.01.165.

[20] Yoo E, Kim M, Song HH. Well-to-wheel analysis of hydrogen fuel-cell electric vehicle in Korea. Int J Hydrogen Energy 2018;43:19267–78. https://doi.org/10.1016/J.IJHYDENE.2018.08.088.

[21] Lee D-Y, Elgowainy A, Vijayagopal R. Well-to-wheel environmental implications of fuel economy targets for hydrogen fuel cell electric buses in the United States. Energy Policy 2019;128:565–83. https://doi.org/10.1016/J.ENPOL.2019.01.021.

[22] Ou X, Zhang X, Chang S. Alternative fuel buses currently in use in China: life-cycle fossil energy use, GHG emissions and policy recommendations. Energy Policy 2010;38:406–18. https://doi.org/10.1016/J.ENPOL.2009.09.031.

[23] Ally J, Pryor T. Life-cycle assessment of diesel, natural gas and hydrogen fuel cell bus transportation systems. J Power Sources 2007;170:401–11. https://doi.org/10.1016/J.JPOWSOUR.2007.04.036.

[24] Lee DY, Elgowainy A, Kotz A, Vijayagopal R, Marcinkoski J. Life-cycle implications of hydrogen fuel cell electric vehicle technology for medium- and heavy-duty trucks. J Power Sources 2018;393:217–29. https://doi.org/10.1016/j.jpowsour.2018.05.012.

[25] Liu F, Zhao F, Liu Z, Hao H. The impact of fuel cell vehicle deployment on road transport greenhouse gas emissions: the China case. Int J Hydrogen Energy 2018;43:22604–21. https://doi.org/10.1016/J.IJHYDENE.2018.10.088.

[26] Huang Z, Zhang X. Well-to-wheels analysis of hydrogen based fuel-cell vehicle pathways in Shanghai. Energy 2006;31:471–89. https://doi.org/10.1016/J.ENERGY.2005.02.019.

[27] Ahmadi P, Kjeang E. Realistic simulation of fuel economy and life cycle metrics for hydrogen fuel cell vehicles. Int J Energy Res 2017;41:714–27. https://doi.org/10.1002/er.3672.

[28] Elgowainy A, Han J, Ward J, Joseck F, Gohlke D, Lindauer A, et al. Current and future United States light-duty vehicle pathways: cradle-to-grave lifecycle greenhouse gas emissions and economic assessment. Environ Sci Technol 2018;52:2392–9. https://doi.org/10.1021/acs.est.7b06006.

[29] Sun P, Young B, Elgowainy A, Lu Z, Wang M, Morelli B, et al. Criteria air pollutant and greenhouse gases emissions from U.S. Refineries allocated to refinery products. Environ Sci Technol 2019;53:6556–69. https://doi.org/10.1021/acs.est.8b05870.

[30] Elgowainy A, Han J, Cai H, Wang M, Forman GS, DiVita VB. Energy efficiency and greenhouse gas emission intensity of petroleum products at U.S. Refineries. Environ Sci Technol 2014;48:7612–24. https://doi.org/10.1021/es5010347.

[31] Energy Systems, Argonne National Laboratory. Hydrogen delivery scenario analysis model (HDSAM). https://hdsam.es.anl.gov/index.php?content=hdsam. [Accessed 16 April 2019].

[32] United States Environmental Protection Agency. Final technical support document – fuel economy labeling of motor vehicle revisions to improve calculation of fuel economy estimates. 2006. EPA420-R-06-017.

[33] Environmental Protection Agency. 600.210–12, https://www.govinfo.gov/content/pkg/CFR-2012-title40-vol31/pdf/CFR-2012-title40-vol31-sec600-210-12.pdf. [Accessed 24 June 2019].

Please cite this article as: Liu X et al., Comparison of well-to-wheels energy use and emissions of a hydrogen fuel cell electric vehicle relative to a conventional gasoline-powered internal combustion engine vehicle, International Journal of Hydrogen Energy, https://doi.org/10.1016/j.ijhydene.2019.10.192